HYDROLOGICAL PROCESSES
Hydrol. Process. **30**, 2754–2772 (2016)
Published online 15 June 2016 in Wiley Online Library
(wileyonlinelibrary.com) DOI: 10.1002/hyp.10910

Impact of antecedent conditions on simulations of a flood in a mountain headwater basin

Xing Fang* and John W. Pomeroy
Centre for Hydrology, University of Saskatchewan, Saskatoon, Canada

Abstract:

A devastating flood struck Southern Alberta in late June 2013, with much of its streamflow generation in the Front Ranges of the Rocky Mountains, west of Calgary. To better understand streamflow generation processes and their sensitivity to initial conditions, a physically based hydrological model was developed using the Cold Regions Hydrological Modelling platform (CRHM) to simulate the flood for the Marmot Creek Research Basin (~9.4 km^2). The modular model includes major cold and warm season hydrological processes including snow redistribution, sublimation, melt, runoff over frozen and unfrozen soils, evapotranspiration, subsurface runoff on hillslopes, groundwater recharge and discharge and streamflow routing. Uncalibrated simulations were conducted for eight hydrological years and generally matched streamflow observations well, with a NRMSD of 52%, small model bias (−3%) and a Nash–Sutcliffe efficiency (NSE) of 0.71. The model was then used to diagnose the responses of hydrological processes in 2013 flood from different ecozones in Marmot Creek: alpine, treeline, montane forest and large and small forest clearings to better understand spatial variations in the flood runoff generation mechanisms. To examine the sensitivity to antecedent conditions, 'virtual' flood simulations were conducted using a week (17 to 24 June 2013) of flood meteorology imposed on the meteorology of the same period in other years (2005 to 2012), or switched with the meteorology of one week in different months (May to July) of 2013. Sensitivity to changing precipitation and land cover was assessed by varying the precipitation amount during the flood and forest cover and soil storage capacity in forest ecozone. The results show that runoff efficiency increases rapidly with antecedent snowpack and soil moisture storage with the highest runoff response to rainfall from locations in the basin where there are recently melted or actively melting snowpacks and resulting high soil moisture or frozen soils. The impact of forest canopy on flooding is negligible, but flood peak doubles if forest canopy removal is accompanied by 50% reduction in water storage capacity in the basin.

KEY WORDS flood; rain-on-snow; antecedent condition; snow; subsurface storage; Canadian Rockies; forest hydrology

Received 1 October 2015; Accepted 3 May 2016

INTRODUCTION

A flood is overflowing water that inundates land which is normally dry and is one of the most common natural hazards that cause severe damages to life and property in many parts of the world (Kron, 2005). The cost of flood damage from 1990s to 2005 worldwide was over USD $250 billion (Kron, 2005), and more than €7 billion damage was caused by European floods in 2002 (Whitfield, 2012). In Canada, floods occur five times as often as other natural disasters and damage estimates are billions of dollars (Sandink *et al.,* 2010). Total cost of the 'flood of the century' in Southern Manitoba was approximately CAD $1 billion, and about 27 400 people were evacuated (Rannie, 2016). The June 2013 flood in Southern Alberta was the costliest natural disaster in Canada, with total damage exceeding CAD $6 billion (Pomeroy *et al.,* 2016a; Simonovic, 2014).

In Canada, flood types are related to regional and landscape settings (Buttle *et al.,* 2016). Snowmelt floods are generated from large winter snow accumulation and rapid melt rates and are common in many regions of Canada (Lawford *et al.,* 1995; Pomeroy *et al.,* 2014; Rannie, 2016; Saad *et al.,* 2016; Stadnyk *et al.,* 2016). Snowmelt floods usually occur during the spring freshet, which can be coupled with heavy rainfall that can result in even more severe flooding because of rain-on-snow processes (Dumanski *et al.,* 2015; Newton and Burrell, 2016). Rain-on-snow floods are common in high elevation coastal regions (Beaudry and Golding, 1983; Marks *et al.,* 1998; Mazurkiewicz *et al.,* 2008; McCabe *et al.,* 2007). In Canada, summer flooding usually arises from local convective rainfall events, but there has been occurrence of floods attributed to frontal precipitation in Prairie (Shook and Pomeroy, 2012) and to large scale convective precipitation in Rocky Mountain foothills

*Correspondence to: Xing Fang, Centre for Hydrology, University of Saskatchewan, 117 Science Place, Saskatoon, Sask. S7N 5C8, Canada.
E-mail: xing.fang@usask.ca

(Pomeroy *et al.,* 2016a; Shook, 2016). In mountainous regions, several mechanisms are responsible for generating floods. Coastal mountain basins in British Columbia usually have snowmelt-induced flood in spring or summer and rainfall or rain-on-snow generated floods in fall or winter (Buttle *et al.,* 2016); rainfall leads to more extreme floods than snowmelt in this region (Melone, 1985). Conversely, heavy rainfall from mesoscale systems is the leading mechanism for floods for the interior mountain regions. Such a mechanism caused flooding in and near Boulder, Colorado in September 2013 (Gochis *et al.,* 2015). In the Canadian Rockies in June 2013, discharge magnitude and volume were increased by melt of the remnant alpine snowpack prior to and during the mesoscale rainfall, in this case both heavy rainfall and rain-on-snow were responsible for triggering catastrophic flooding (Liu *et al.,* 2016; Pomeroy *et al.,* 2016a).

Mountains are characterized by highly variable depth and phase of precipitation because of temperature gradients and orography (Lundquist and Cayan, 2007; Marks *et al.,* 2013), and slope and aspect are factors influencing snow accumulation and melt patterns (DeBeer and Pomeroy, 2009; MacDonald *et al.,* 2010; Marsh *et al.,* 2012; Poulos *et al.,* 2012) and evaporative loss. Spatial extent, type and forest canopy structure are other factors controlling the heterogeneity of radiation energy, interception loss, snowmelt rate, subsurface water storage, evapotranspiration and runoff in mountains (Band, 1993; Ellis *et al.,* 2011, 2013; Musselman *et al.,* 2008; Pomeroy *et al.,* 2009, 2012). These biophysical factors control the streamflow response to precipitation inputs to mountain basins (Hunsaker *et al.,* 2012; Zhang and Wei, 2014). With spatially variable hydrological processes in mountain regions, predicting floods is a difficult task because of lack of knowledge about the complexity and rapidity of hydrological response to flood (de Jong, 2013). While field studies have been conducted to improve the understanding of spatial and temporal runoff generation during rain-on-snow (ROS) flooding in the Black Forest region of Germany (Garvelmann *et al.,* 2015), such field studies can rarely be accomplished as observation stations are often destroyed during floods. It is therefore important for a hydrological model to have the ability to simulate flood processes in mountain regions. The physically based hydrological model CRHM (Pomeroy *et al.,* 2007) has been developed from understanding gained in field studies (DeBeer and Pomeroy, 2010; Ellis and Pomeroy, 2007; Ellis *et al.,* 2013; MacDonald *et al.,* 2010; Pomeroy *et al.,* 2009) and has simulated hydrological processes and runoff generation in mountain headwater basins (Fang *et al.,* 2013; Pomeroy *et al.,* 2013). The objectives of this paper are to use CRHM simulations to: (1) diagnose flood generation processes and their spatial variations, (2) examine flood discharge sensitivity to antecedent conditions of precipitation, air temperature, snowpack and subsurface storages, and (3) examine flood discharge sensitivity to magnitude of precipitation event, forest cover and soil moisture storage capacity.

METHODOLOGY

Study site and field observations

The study was conducted in the Marmot Creek Research Basin (MCRB) (50°57′N, 115°09′W) in the Kananaskis Valley, Alberta, Canada, located within the Front Ranges of the Canadian Rocky Mountains (Figure 1). MCRB is a small headwater basin (9.4 km^2) of the Bow River basin and flows into the Kananaskis River. Elevation ranges from 1590 m.a.s.l at the Marmot Creek outlet to 2829 m.a.s.l at the summit of Mount Allan. MCRB is partly covered by needleleaf vegetation that is dominated by Engelmann spruce (*Picea engelmanni*) and subalpine fir (*Abies lasiocarpa*) in the upper part of basin (1710 to 2277 m.a.s.l); the lower elevation (1590 to 2015 m.a.s.l) forests are mainly Engelmann spruce and lodgepole pine (*Pinus contorta* var. Latifolia) with small coverage of aspen presented near the basin outlet (Kirby and Ogilvy, 1969). Forest management experiments in the 1970s and 1980s left large clear-cutting blocks (1838 to 2062 m.a.s.l) in the Cabin Creek sub-basin and a series of small circular clearings (1762 to 2209 m.a.s.l) in the Twin Creeks sub-basin (Golding and Swanson, 1986). Exposed rock surface and talus are present in the high alpine part of basin (1956 to 2829 m.a.s.l); alpine larch (*Larix lyallii*) and short shrub are present around the treeline at approximately 2016 to 2379 m.a.s.l. Physiographic descriptions of these ecozones are listed in Table I. The surficial soils are primarily poorly developed mountain soils consisted of glaciofluvial and till surficial deposits (Beke, 1969). Relatively impermeable bedrock is found at the higher elevations and headwater areas, and the rest of basin is covered by a deep layer of coarse and permeable soil allowing for rapid rainfall infiltration to deep subsurface layers (Jeffrey, 1965). Continental air masses control the weather in the region, which has long and cold winters and cool and wet springs with a late spring/early summer precipitation maximum. Westerly warm and dry Chinook (foehn) winds lead to brief periods with the air temperature above 0 °C during the winter months. Annual precipitation ranges from 600 mm at lower elevations to more than 1100 mm at the higher elevations, of which approximately 70 to 75% occurs as snowfall with the percentage increasing with elevation (Storr, 1967). Mean monthly air temperature ranges from 14 °C observed at 1850 m.a.s.l in July to −10 °C observed at 2450 m.a.s.l in January.

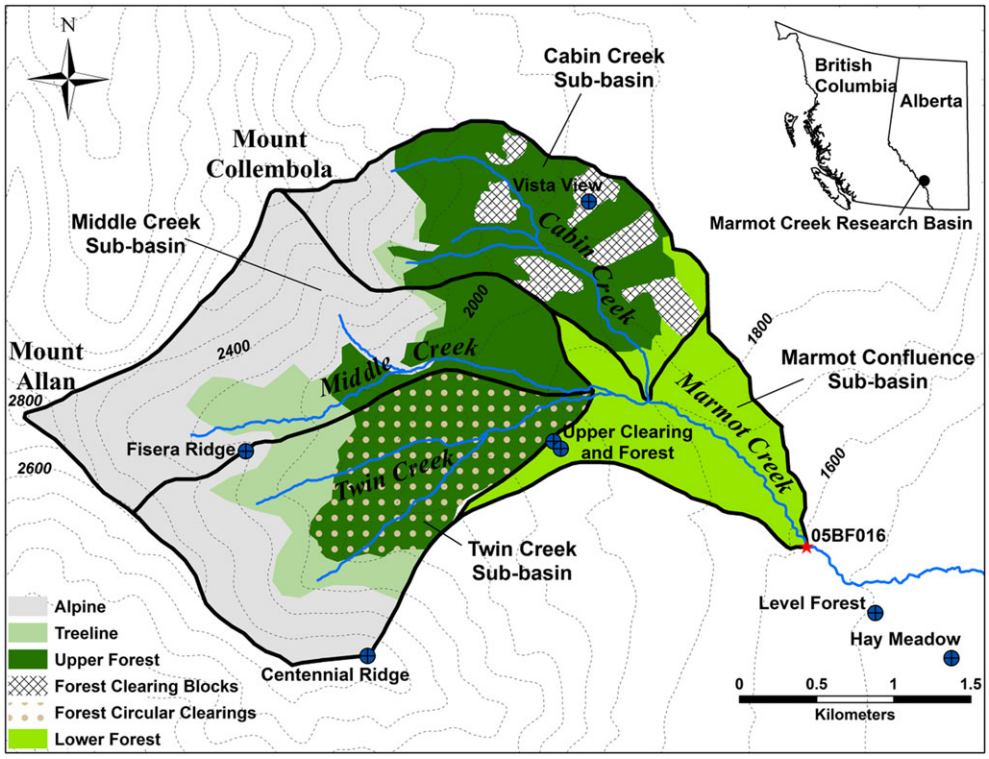

Figure 1. Location and contour map (m) of the Marmot Creek Research Basin (MCRB), showing hydrometeorological (blue cross circles) and streamflow stations (red star), and ecozones of the MCRB: alpine, treeline, upper forest, forest clearing blocks, forest circular clearings, and lower forest. Note that the area where there are small clearings is shown, but individual clearings are too small to be shown at this scale

Table I. Area and mean elevation, aspect and slope for ecozones at the Marmot Creek Research Basin. Note that the aspect is in degree clockwise from North

Ecozone	Area (km^2)	Area (% of basin)	Elevation (m a.s.l)	Aspect (°)	Slope (°)
Alpine	3.23	34.5	2413	110	30
Treeline	0.93	10.0	2217	91	22
Upper Forest	2.75	29.3	1983	108	20
Forest Clearing Blocks	0.40	4.3	1927	140	11
Forest Circular Clearing North-facing	0.26	2.7	1966	34	17
Forest Circular Clearing South-facing	0.24	2.6	2014	113	21
Lower Forest	1.42	15.2	1756	113	14

Model forcing meteorological observations of air temperature, relative humidity, wind speed, precipitation, soil temperature and incoming short-wave radiation were collected from the Centennial Ridge, Fisera Ridge, Vista View, Upper Clearing and Upper Forest, Level Forest and Hay Meadow hydrometeorological stations. These stations are shown in Figure 1 and are described in several publications (DeBeer and Pomeroy, 2010; Ellis *et al.,* 2010; MacDonald *et al.,* 2010). Precipitation was measured with an Alter-shielded Geonor weighing precipitation gauge at Hay Meadow, Upper Clearing and Fisera Ridge and was corrected for wind-induced undercatch. Meteorological data were spatially distributed from observations stations across the basin with adjustments for temperature by a constant environmental lapse rate (0.75 °C/100 m) and adjustments for precipitation based on observed seasonal gradients from several years of observations at multiple elevations. Because of the high density of stations at multiple elevations, the distributed meteorology is not sensitive to lapse rates and precipitation gradients chosen. Vapour pressure was conserved for unsaturated conditions and not allowed to exceed saturation vapour pressure when extrapolated. Radiation inputs were adjusted for slope and sky view using the various methods described by Fang *et al.* (2013). Environment Canada's Water Survey of Canada maintains a long-term streamflow gauge (05BF016) at the Marmot Creek basin outlet shown in Figure 1, providing

seasonal (1 May–31 October) daily mean streamflow discharge from hourly stage measurements with a well-established rating curve (Bruce and Clark, 1965). For 2013, the gauge provided data through 18 June but was destroyed by a debris torrent in the flood; as a result, no reliable stage data were recorded after the flood began. However, a highly uncertain peak flow estimate of between 2.8 and 3.2 m^3/s was made by Harder *et al.* (2015) by regressing the measured discharge at the surviving Upper Marmot Creek gauge to the basin outlet gauge before the outlet gauge was destroyed.

Model description

The Cold Regions Hydrological Modelling platform (CRHM) was used to develop a hydrological model for MCRB. CRHM is an object-oriented, modular and flexible platform for assembling physically based hydrological models. With CRHM, the user constructs a purpose-built model from a selection of possible basin spatial configurations, spatial resolutions and physical process modules of varying degrees of physical complexity. Basin discretization is performed via dynamic networks of hydrological response units (HRUs) whose number and nature are selected based on the variability of basin attributes and the level of physical complexity chosen for the model. Physical complexity is selected by the user in light of hydrological understanding, parameter availability, basin complexity, meteorological data availability and the objective flux or state for prediction. A full description of CRHM is provided by Pomeroy *et al.* (2007). For the MCRB, a set of physically based modules was constructed to simulate the dominant hydrological processes by Pomeroy *et al.* (2012) and Fang *et al.* (2013). Since that model setup, updates have been made to the evaporation and hillslope modules. While the hillslope modification is important for snowmelt runoff and is described by Pomeroy *et al.* (2016b), the evaporation module change is important for calculating antecedent soil moisture conditions and is described here. For actual evaporation estimation of unsaturated surfaces, Granger's evapotranspiration expression (Granger and Gray, 1989) was replaced by the Penman–Monteith (P–M) evapotranspiration algorithm (Monteith, 1965)

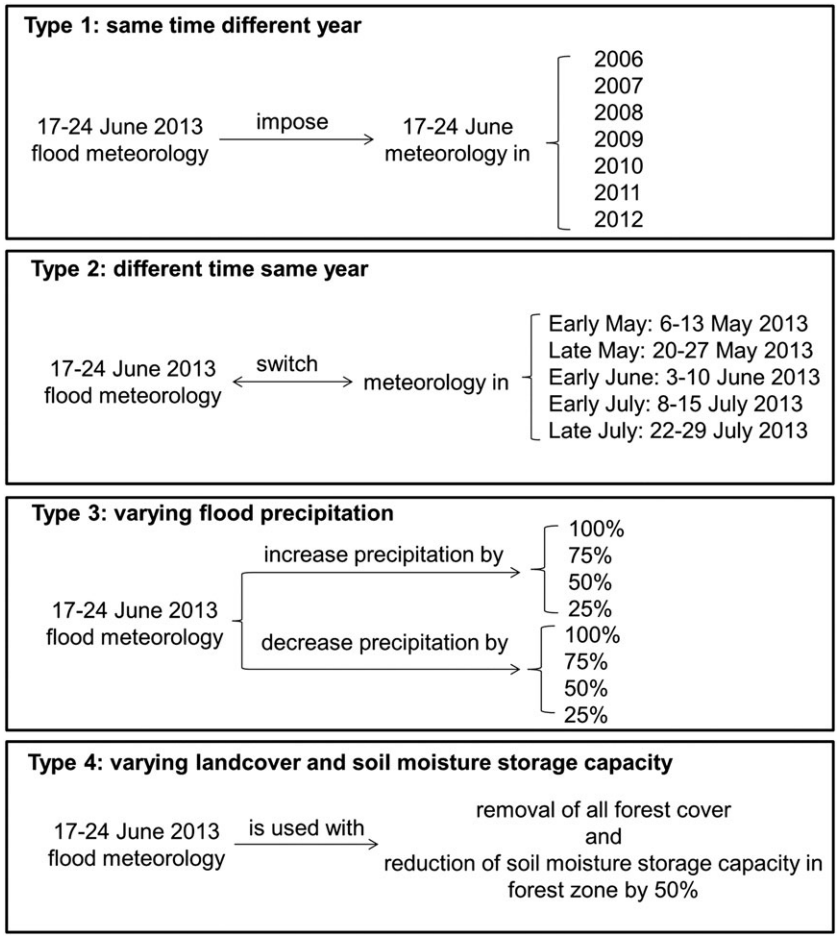

Figure 2. Flood simulation scheme

with a Jarvis-style resistance formulation (Verseghy, 1991). The P–M method includes stomatal and aerodynamic resistances which control water vapour transfer to the atmosphere, representing the diffusion path lengths through vegetation and the boundary layer, respectively. Stomatal resistance varies with the biophysical properties of vegetation (i.e. leaf area index, plant height, rooting zone) and is affected by four environmental stress factors: light limitation, vapour pressure deficit, soil moisture tension or air entry pressure, and air temperature. This update enables a more realistic representation of the evaporation process for vegetation with seasonal variations of leaf area index and plant height (i.e. alpine shrub, alpine larch, aspen).

Flood simulations

To examine the effects of antecedent conditions, magnitude of precipitation, forest cover and soil storage capacity on flood discharge, the meteorology observed at MCRB during 17–24 June 2013 was used for simulations with modifications described below. During this period, approximately 250-mm total precipitation was measured in the basin (Pomeroy *et al.,* 2016a). Four types of flood simulations were conducted, which are summarized as follows and is illustrated in Figure 2:

Type 1, same time different year: impose the meteorology of 17–24 June 2013 on the same time period (i.e. 17–24 June) in other seven years: from 2006 to 2012.

Type 2, different time same year: switch the meteorology of 17–24 June 2013 with meteorology in different time periods of 2013: early May (6–13 May), late May (20–27 May), early June (3–10 June), early July (8–15 July) and late July (22–29 July).

Type 3, varying flood precipitation: increase and decrease the precipitation of 17–24 June 2013 by: from 25% to 100%.

Type 4, varying landcover and soil moisture storage capacity: remove all forest cover and then reduce soil moisture storage capacity in the forest zone by 50%.

In total, there are 23 flood simulations that are summarized in Table II.

RESULTS

Model evaluation

To assess the model reliability, streamflow simulations were compared to observed outlet discharge at the Water Survey of Canada gauge (Figure 3). The simulation provides information on all the hydrological processes for runoff generation and streamflow routing at the basin scale. The gauged flow extended from 1 May to 30 September during 2006–2012 and for part of 2013 before the flood. Table III lists Nash–Sutcliffe efficiency (NSE) (Nash and Sutcliffe, 1970) and other model evaluation

Table II. Description of the flood simulations at the Marmot Creek Research Basin

Flood simulation	Description
1	impose 17–24 June 2013 meteorology to 17–24 June 2006
2	impose 17–24 June 2013 meteorology to 17–24 June 2007
3	impose 17–24 June 2013 meteorology to 17–24 June 2008
4	impose 17–24 June 2013 meteorology to 17–24 June 2009
5	impose 17–24 June 2013 meteorology to 17–24 June 2010
6	impose 17–24 June 2013 meteorology to 17–24 June 2011
7	impose 17–24 June 2013 meteorology to 17–24 June 2012
8	switch meteorology between 17–24 June 2013 and 6–13 May 2013
9	switch meteorology between 17–24 June 2013 and 20–27 May 2013
10	switch meteorology between 17–24 June 2013 and 3–10 June 2013
11	switch meteorology between 17–24 June 2013 and 8–15 July 2013
12	switch meteorology between 17–24 June 2013 and 22–29 July 2013
13	increase precipitation in 17–24 June 2013 by 100%
14	increase precipitation in 17–24 June 2013 by 75%
15	increase precipitation in 17–24 June 2013 by 50%
16	increase precipitation in 17–24 June 2013 by 25%
17	decrease precipitation in 17–24 June 2013 by 25%
18	decrease precipitation in 17–24 June 2013 by 50%
19	decrease precipitation in 17–24 June 2013 by 75%
20	decrease precipitation in 17–24 June 2013 by 100%
21	remove all forest cover
22	remove all forest cover and reduce soil moisture storage capacity in forest zone by 50%
23	actual 17–24 June 2013 flood

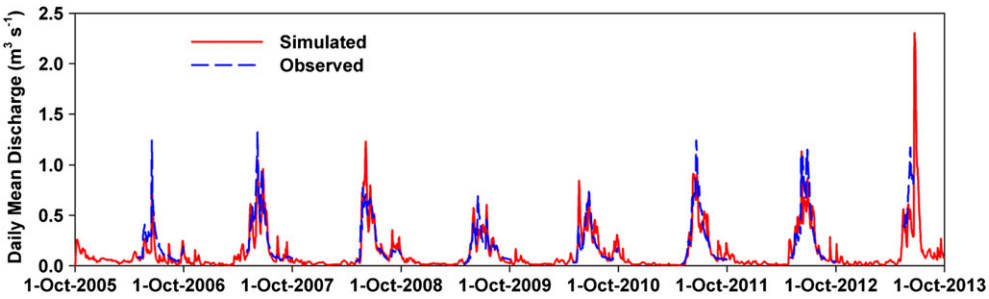

Figure 3. Comparisons of observed and simulated daily streamflow for 2005–2013 for Marmot Creek. Observations were not available for Marmot Creek during the 2013 flood because of gauge damage

Table III. Evaluation of the simulated daily mean streamflow discharge for Marmot Creek using the Nash–Sutcliffe efficiency (NSE), root mean square difference (RMSD, $m^3\ s^{-1}$), normalized RMSD (NRMSD) and model bias (MB)

	NSE	RMSD	NRMSD	MB	MB (peak discharge)	RMSD (peak discharge)
2006	0.63	0.117	0.60	−0.39	−0.32	
2007	0.77	0.141	0.47	−0.09	−0.21	
2008	0.63	0.134	0.50	0.11	0.58	
2009	0.61	0.093	0.47	−0.01	−0.13	
2010	0.50	0.131	0.64	0.22	0.15	
2011	0.77	0.136	0.48	−0.02	−0.26	
2012	0.75	0.164	0.52	−0.08	−0.02	
All seasons	0.71	0.133	0.52	−0.03	−0.07	0.28

indexes—root mean square difference (RMSD), normalized RMSD (NRMSD) and model bias (MB) calculated by equations shown in Fang *et al.* (2013). The seasonal NSE ranged from 0.5 in 2010 to 0.77 in 2007 and 2011, with value of 0.71 over seven seasons. This indicates that model was able to predict the temporal evolution of daily basin discharge in this period. The RMSD, NRMSD and MB were $0.133\ m^3\ s^{-1}$, 0.52 and −0.03 for the simulated daily basin discharge, respectively, suggesting small differences between the simulation and observation of Marmot Creek basin daily discharge. The RMSD and MB were $0.28\ m^3\ s^{-1}$ and −0.07 for the estimated peak daily basin discharge during 2006–2012, indicating that simulated peak daily discharge was comparable to the measured value. For 2013, the simulated peak daily discharge of $2.45\ m^3\ s^{-1}$ during the flood was lower than the Harder *et al.* (2015) estimate by 0.35 to $0.75\ m^3\ s^{-1}$—how much of this difference is measurement error or model error is unknown.

To provide further evaluation of model process function, snow accumulation and snowmelt simulations were evaluated against the observations at the mature forest, forest clearing, alpine slope and treeline sites during 2007–2013 (Table IV). Overall, the model was able to capture the seasonal snow accumulation and melt, with relative low values of MB for all six seasons, ranging from 0.08 for the forest clearing to 0.20 for the larch forest treeline. The RMSD ranged from 31.1 mm for the mature spruce forest to 172.1 mm for the larch forest treeline, while the NRMSD ranged from 0.28 for the lower alpine south slope to 0.56 for the mature spruce forest.

Flood generation mechanisms

Mechanisms for generating the 2013 flood in the basin included snowmelt, rain-on-snow (ROS) and rainfall. Snowmelt-generated flood is because of the melting of large accumulated snowpack, and rainfall-driven flood is result of heavy rain from mesoscale convective system. ROS-flood is generated by rapid snowmelt enhanced by large amount of rainfall. Figure 4(a) and (b) shows the time series of runoff and storage change for the major ecozones. The 2013 flood was primarily generated from higher elevations; 72% of total basin flow volume was from alpine and treeline ecozones which cover about 45% of the basin. At lower elevations there is substantial storage capacity and unfrozen soils—here initial precipitation fills storage until runoff can be produced to contribute to discharge. At higher elevations soils have diminished storage capacity because of higher volumetric soil moisture contents, frozen conditions and thinner layers—here runoff is generated quickly and more precipitation goes into runoff and less into storage than at lower elevations. Figure 4(c) and (d) shows at the treeline ecozone there is an antecedent snowpack, and so

Table IV. Evaluation of simulated snow accumulation using the root mean square difference (RMSD, mm SWE), normalized RMSD (NRMSD) and model bias (MB) at the Upper Forest/Clearing and Fisera Ridge sites, Marmot Creek Research Basin

	Upper Forest/Clearing		Fisera Ridge	
	Spruce Forest	Forest Clearings	Lower Alpine South-facing Slope	Larch Forest Treeline
			RMSD	
2007–2008	19.3	37.1	48.5	65.1
2008–2009	25.7	21.1	63.2	75.3
2009–2010	22.2	38.6	291.3	372.1
2010–2011	12.0	69.0	105.0	132.4
2011–2012	31.5	22.7	96.3	147.4
2012–2013	52.4	66.3	110.6	146.4
All seasons	31.1	45.1	131.5	172.1
			NRMSD	
2007–2008	0.49	0.37	0.09	0.10
2008–2009	0.64	0.26	0.16	0.19
2009–2010	0.81	0.47	0.87	1.06
2010–2011	0.13	0.45	0.29	0.33
2011–2012	0.47	0.16	0.16	0.23
2012–2013	0.75	0.44	0.24	0.30
All seasons	0.56	0.37	0.28	0.34
			MB	
2007–2008	−0.44	−0.22	−0.06	0.03
2008–2009	−0.53	0.03	−0.02	0.14
2009–2010	−0.29	−0.40	0.86	0.97
2010–2011	−0.01	0.39	0.26	0.29
2011–2012	−0.40	0.03	0.13	0.12
2012–2013	0.64	0.41	0.07	0.15
All seasons	−0.10	0.08	0.14	0.20

ROS is generated with runoff produced both from ROS and snowmelt. ROS is a highly efficient runoff generation mechanism that is examined in detail by Pomeroy *et al.* (2016b). ROS runoff is stored as detention flow in the deeper snowpacks but generally flows quickly as overland flow to form streamflow. At higher elevations (i.e. alpine and treeline ecozones), the last component of precipitation during the flood (9%) fell as snowfall and melted over the next few days, causing a substantial delay in runoff generation and a shift from rainfall–runoff and ROS runoff to snowmelt runoff at the end of the heavy precipitation period and for several days afterwards.

Flood simulation of same time different year

Streamflow discharge and total subsurface storage in soil and groundwater layers over the basin were simulated given the substitution of the 17–24 June 2013 flood meteorology for the same period (17–24 June) in seven previous years (2006 to 2012). Figure 5 shows simulations of hourly discharge with and without the flood meteorology for these seven hydrological years as well as the flood year of 2012–2013. With observed pre-flood meteorology, the simulated annual peak discharge ranged from $0.86\,m^3\,s^{-1}$ at 0300 h 22 May 2010 to $1.34\,m^3\,s^{-1}$ at 1700 h 4 June 2008; with the synthetic flood meteorology, the simulated annual peak discharge increased dramatically, ranging from $2.62\,m^3\,s^{-1}$ at 2100 h 21 June 2009 to $3.15\,m^3\,s^{-1}$ at 2100 h 21 June 2011. The simulated peak discharge for the June 2013 flood was $2.57\,m^3\,s^{-1}$ at 2100 h 21 June 2013, which is lower than any of the other peaks simulated by substitution. Figure 5 also shows the simulated subsurface storage dynamics with and without substitution of flood meteorology. Without the flood meteorology, the estimated peak subsurface storage as fraction of saturation in the seven hydrological years ranged from 48.3% at 0300 h 16 June 2006 to 67.5% at 0400 h 19 June 2011. This increased substantially with the substitution in flood meteorology where peak subsurface storage ranged from 59.2% of saturation at 2000 h 22 June 2006 to 74% at 2000 h 22 June 2011, while the simulated peak subsurface storage reached 62.6% of saturation at 2300 h 22 June for the June 2013 flood. Clearly one of the implications of the heavy rainfall was an increase in storage, partially diverting water from runoff formation and streamflow generation; however, how much was stored varied from year to year.

Relationships between flood runoff and antecedent conditions were examined for all ecozones shown in Figure 1 as well as for the entire Marmot Creek basin

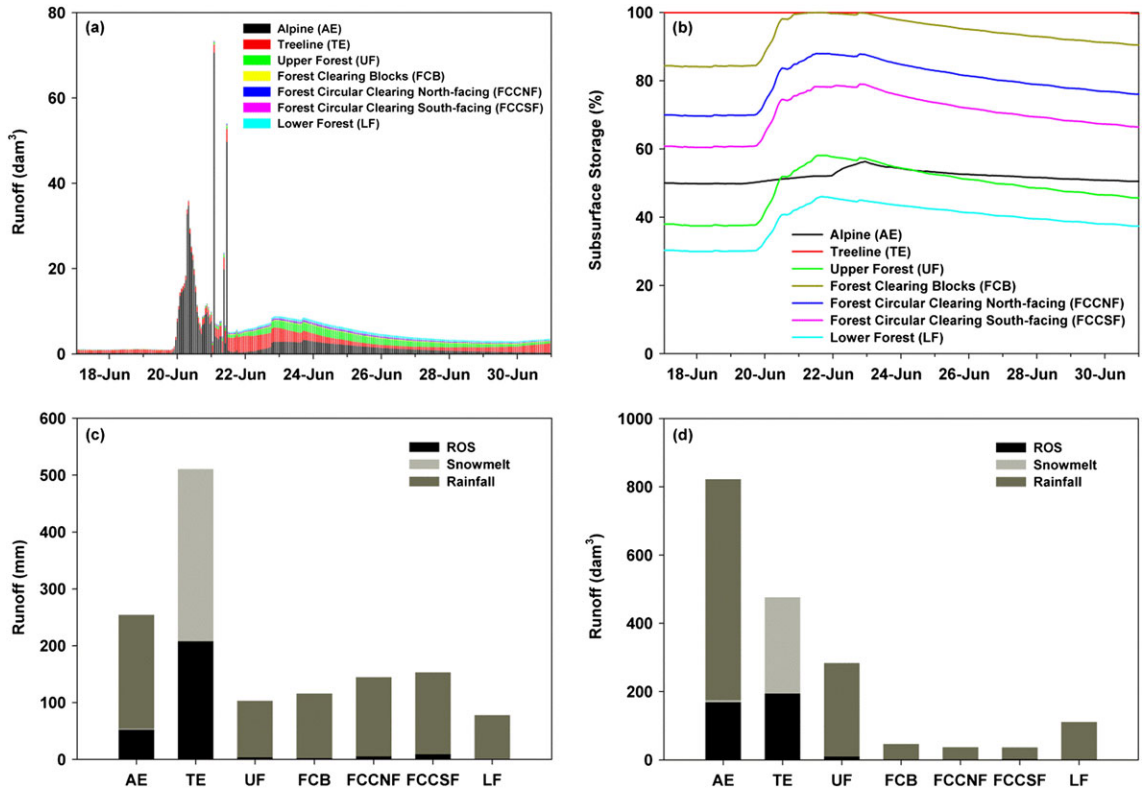

Figure 4. Model simulation of flood generation mechanisms during 17–30 June 2013: (a) time series of runoff contribution of each ecozone to basin discharge, (b) time series of subsurface storage in each ecozone, (c) total unit runoff (mm) generation mechanism for each ecozone and (d) total runoff (dam^3) generation mechanism contribution of each ecozone to basin discharge

using simulations from the flood substitution technique and real meteorology over eight hydrological years from 2005–2006 to 2012–2013. Flood runoff is considered to be the total runoff during the two-week period of 17–30 June in each hydrological year. A flood generation efficiency (FGE) is defined as this two-week discharge divided by the storm event precipitation of 250 mm and was compared to antecedent conditions such as precipitation, air temperature, soil saturation and snowpack for each year. A FGE >1.0 indicates more discharge volume is generated than the storm precipitation volume, while a FGE <1.0 indicates less discharge volume than storm precipitation volume (in this case <250 mm equivalent depth of discharge over the basin). Antecedent precipitation is the total precipitation from the beginning of the hydrological year to the onset of the flood (i.e. 1 October–17 June); antecedent air temperature is the average air temperature in June prior to onset of flood (i.e. 1–17 June), and antecedent soil saturation and snowpack are the pre-flood soil saturation and snow accumulation on 17 June, respectively. Figure 6 illustrates the scatter plots of FGE and antecedent conditions for all ecozones and the entire basin. The Pearson correlation coefficient r was calculated for these associations and is shown in Table V. A two-tailed test with significance level of 0.05 was conducted for the calculated r. The results show significant positive correlations between the FGE and antecedent precipitation only for the large forest clearings ($r=0.75$) and lower forest ($r=0.79$) and between FGE and antecedent soil saturation for all ecozones with r ranging from 0.73 to 0.97 except for the lower forest ($r=0.56$), while FGE was only significantly and negatively correlated with antecedent air temperature for alpine ($r=-0.73$) where a snowpack or recent snowpack is possible in colder years. For the snowpack, however, the Pearson correlation coefficient was only 0.37 and 0.29 for alpine and treeline zones, indicating an insignificant positive correlation between the FGE and antecedent snowpack; r was not calculated for other ecozones because of lack of antecedent snowpack.

Figure 6 shows differing runoff generation mechanisms between ecozones above and below the treeline. Rainfall–runoff was the sole mechanism for generating runoff during the flood for ecozones below the treeline, where the FGE was less than 1.0 in all years, except for the north-facing forest circular clearing ecozone in 2011 (FGE $=1.03$) where antecedent soil saturation was 82%, higher than other years. For treeline and alpine, rain-on-snow (ROS) and snowmelt were responsible for runoff

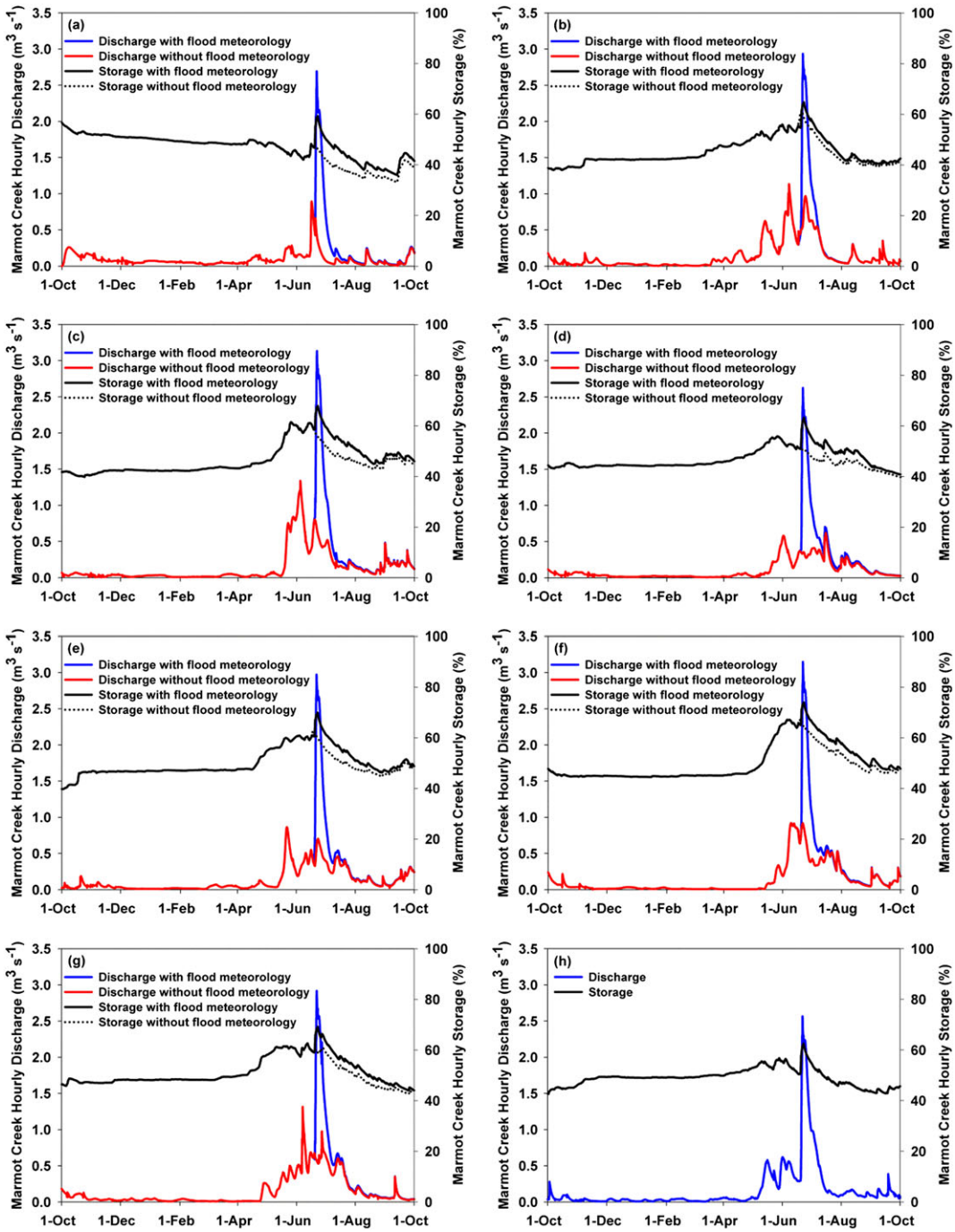

Figure 5. Hourly basin discharge and total subsurface storage from flood simulations of the same time but different year using the flood meteorology of 17–24 June 2013 to same period (17–24 June) in other hydrological years: (a) 2005–2006, (b) 2006–2007, (c) 2007–2008, (d) 2008–2009, (e) 2009–2010, (f) 2010–2011, and (g) 2011–2012; (h) shows the simulated hourly basin discharge and total subsurface storage in 2012–2013 with actual meteorology

generation during and immediately after the flood, with FGE greater than 1.0 in all years. Because of the different runoff generation mechanisms, the Pearson correlation coefficient r was calculated for associations between variables drawn from the combined ecozones below treeline and combined ecozones of treeline and alpine. Below treeline, there are significant positive correlations between FGE and antecedent precipitation ($r = 0.63$) and between FGE and antecedent soil saturation ($r = 0.83$), but significant negative correlations between FGE and antecedent air temperature ($r = -0.54$). At and above treeline, the FGE was only significantly correlated with

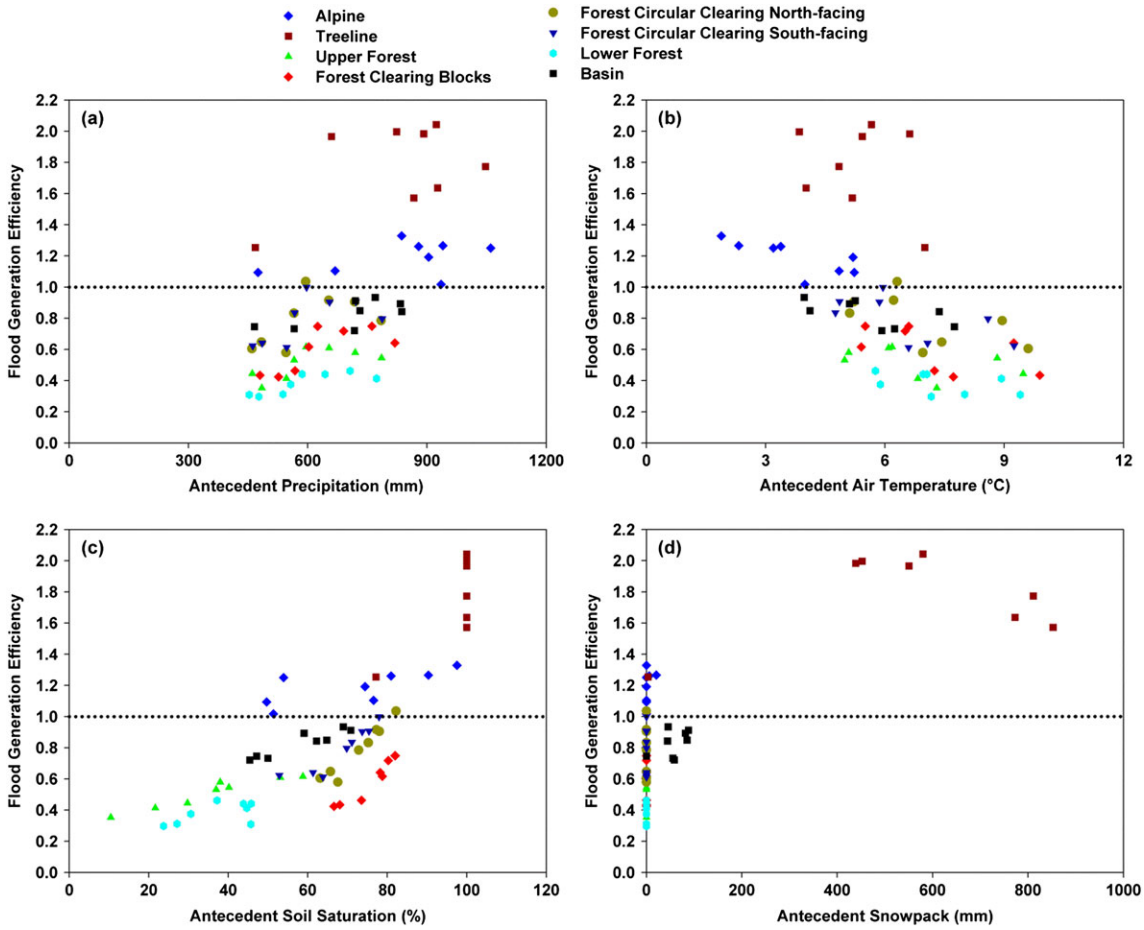

Figure 6. Scatter plots of the flood generation efficiency (FGE) and antecedent conditions from flood simulations of same time different year in eight hydrological years 2005–2013: (a) antecedent precipitation, (b) antecedent air temperature, (c) antecedent soil saturation, and (d) antecedent snowpack. Note FGE is the flood runoff divided by event precipitation of 250 mm and the black dotted line denotes FGE = 1

Table V. Pearson correlation coefficient r for correlation between the flood generation efficiency (FGE) and antecedent conditions: precipitation, air temperature, soil saturation, and snowpack as well as correlation between the FGE and storage change from flood simulations of same time different year in eight hydrological years 2005–2013

	Alpine	Treeline	Upper Forest	Forest Clearing Blocks	Forest Circular Clearing North-facing	Forest Circular Clearing South-facing	Lower Forest	Marmot Creek Basin	Below Treeline	Treeline and Alpine
Antecedent precipitation	0.41	0.49	0.67	**0.75**	0.55	0.59	**0.79**	0.66	**0.63**	0.43
Antecedent air temperature	**−0.73**	−0.28	−0.44	−0.57	−0.58	−0.59	−0.47	−0.62	**−0.54**	−0.37
Antecedent soil saturation	**0.73**	**0.77**	**0.95**	**0.97**	**0.97**	**0.93**	0.56	**0.93**	**0.83**	**0.65**
Antecedent snowpack	0.37	0.29						0.47		0.28
Storage change	−0.70	0.56	**−0.81**	**−0.90**	**−0.92**	**−0.91**	−0.53	**−0.71**	**−0.88**	0.26

Note: the **bold** values are statistically significant using two-tailed test with significance level of 0.05.

antecedent soil saturation ($r = 0.65$). This suggests that the impact of antecedent precipitation is not so important in this high precipitation elevation band and that temperature may have a mixed impact because of the effect on snowpack ripeness, remaining snowpack, frozen ground and soil moisture.

The relationship between FGE and change in subsurface storage was explored for all ecozones and entire basin over the eight hydrological years (Figure 7). The subsurface storage change is the total storage in soil and groundwater layers on 30 June minus that on 17 June; positive value means a gain in the storage while negative value suggests a loss in the storage. Table V lists the calculated Pearson correlation coefficient r for these plots and highlights r that passes the two-tailed test with significance level of 0.05. The results show negative correlations between the FGE and storage change for almost all ecozones and the entire basin with r ranging from −0.92 to −0.53. The exception was at the treeline ecozone ($r = 0.56$) where restricted infiltration because of snowpacks and wet and frozen soils resulted in no storage change or drainage during flood events. For combined ecozones below treeline, the value of r was −0.88, implying a significant negative correlation between the FGE and storage change. For the treeline and above, there was an insignificant correlation ($r = 0.26$) between FGE and storage change because of snowpack, frozen soils and presence of exposed bedrock. All ecozones except for treeline demonstrated a classic relationship between runoff and storage change; that is, runoff decreased when storage change increased, which was enhanced by lower antecedent storage condition. For the treeline ecozone, the non-classic relationship between runoff and storage change is attributed to ROS runoff generation from the large antecedent snowpack and restricted infiltration because of wet or frozen soils. In the classic relationship, runoff is inversely related to storage change, while in the non-classic relationship, runoff is neither directly nor inversely related to storage change.

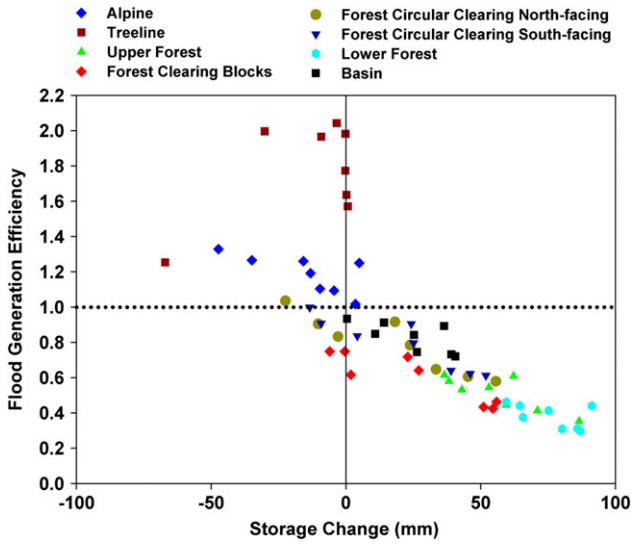

Figure 7. Scatter plots of the flood generation efficiency (FGE) and subsurface storage change from flood simulations of same time different year in eight hydrological years 2005–2013. Note FGE is the flood runoff divided by event precipitation of 250 mm, and the black dotted line denotes FGE = 1

Flood simulation for different dates in 2013

By switching the 17–24 June 2013 flood meteorology with five other time periods in 2013 from early May to late July, streamflow discharge and total subsurface storage in soil and groundwater layers were simulated for Marmot Creek basin on an hourly basis and compared to 'unswitched' conditions (Figure 8). The estimated hourly peak basin discharge ranged from a high of 2.91 $m^3 s^{-1}$ at 2100 h 10 May to a low of 2.2 $m^3 s^{-1}$ at 2100 h 26 July; these compare to 2.57 $m^3 s^{-1}$ at 2100 h 21 June because of the actual June 2013 flood. The results suggest that the peak flood discharge could have been 13% higher if the flood occurred in early May (i.e. 6–13 May) and could have been 14% lower if it occurred in late July (i.e. 22–29 July). Therefore, seasonality of the high precipitation event was important. Differences were also found in basin storage, which was higher in the early periods compared to later periods, with peaks ranging from a high of 66% at 2300 h 11 May to a low of 59% at 2300 h 27 July. This means that basin has more available storage capacity to absorb flood precipitation in later periods such as July when the pre-flood storage is lower because of summer evapotranspiration.

Based on the flood simulations of six different time periods in 2013, relationships between FGE and antecedent conditions of soil saturation and snowpack were examined for all ecozones as well as for the entire basin. FGE was calculated using the 250-mm precipitation and the discharge during the two-week time periods in 2013, defined as 6–19 May for early May, 20 May–2 June for late May, 2–16 June for early June, 17–30 June for late June, 8–22 July for early July and 22 July–4 August for late July. Antecedent soil saturation and snowpack are the immediate pre-flood soil saturation and snowpack accumulation, respectively. Figure 9 shows FGE plotted against antecedent conditions for all ecozones and the entire basin. The Pearson correlation coefficient r for these associations is shown in Table VI, with a highlighted r values significant at $p = 0.05$. FGE was positively correlated with antecedent soil saturation, with r ranging from 0.49 for north-facing forest circular clearing to 0.99 for upper forest and the whole basin; the correlation was significant for the entire basin and most ecozones except for the alpine and the forest circular clearings. There was pre-flood snowpack in alpine and treeline ecozones which sustained significant positive correlations between FGE and antecedent snowpack; these associations scaled up to the basin where they were also significant ($r = 0.89$).

FGE was also correlated to changes in subsurface storage in a similar manner (Figure 10). The subsurface storage change is the change of total storage in soil and

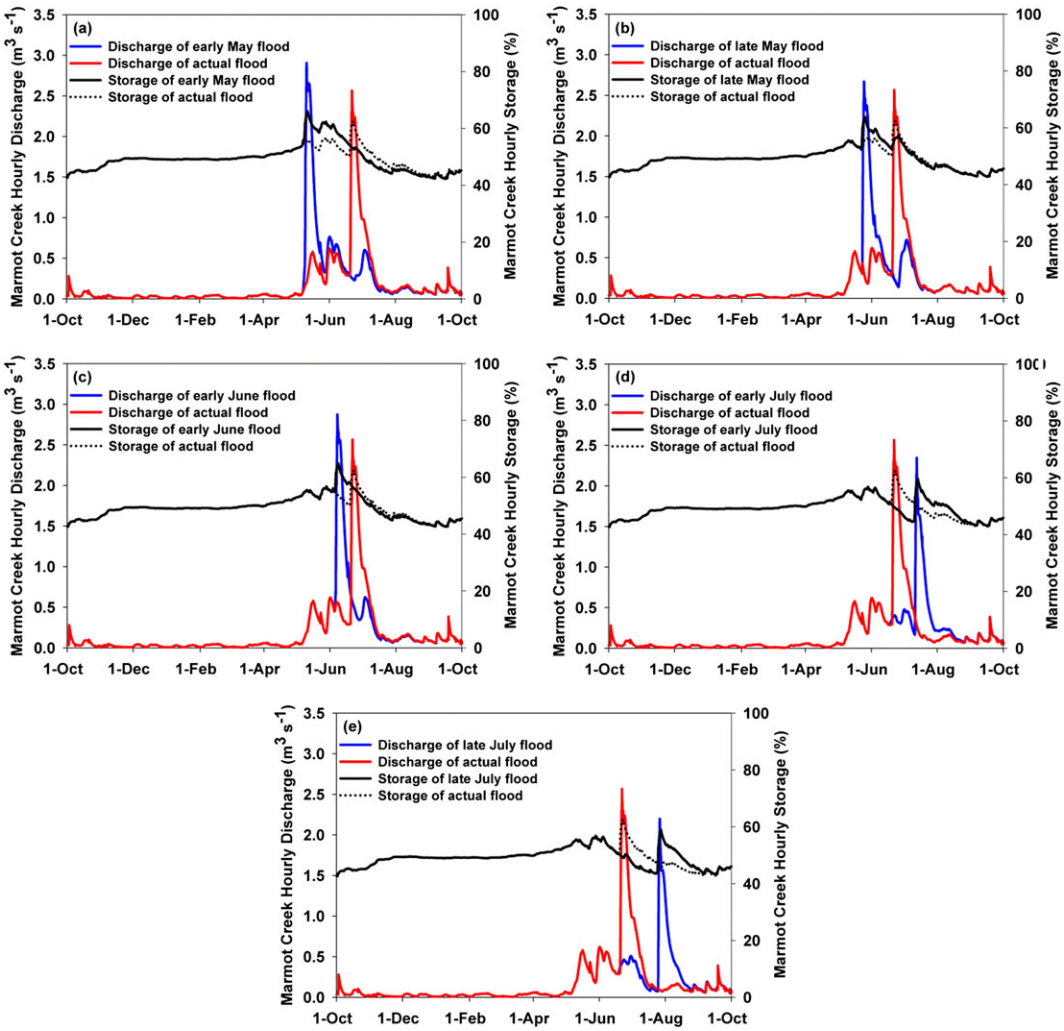

Figure 8. Hourly basin discharge and total subsurface storage from flood simulations of switching the flood meteorology of 17–24 June with five different time periods in 2013: (a) early May, (b) late May, (c) early June, (d) early July, and (e) late July. Red solid and black dot lines show the simulated hourly basin discharge and total subsurface storage in 2012–2013 with actual meteorology (i.e. late June flood)

groundwater layers during the two-week switched flood period. There were significant negative correlations between the FGE and storage change for upper forest, forest clearing blocks, and lower forest as well as the entire basin with r ranging from −0.85 to −0.99 (Table VI), suggesting a classic runoff and storage relationship in the lower basin that scaled to the whole basin. For alpine, treeline and forest circular clearings, FGE was not significantly correlated with storage change, which may have reflected the dominant role of the ROS runoff generation mechanism in early May for alpine and forest circular clearings and in all time periods except for late July for the treeline ecozone.

Flood simulation of varying precipitation magnitude

Streamflow discharge and FGE for Marmot Creek basin were simulated for changing precipitation magnitude scenarios during 17–24 June 2013, from decreasing precipitation by 100% to increasing it by 100% (Figures 11 and 12). A 100% increase is extreme and puts the precipitation volume in the range of that measured for the Boulder, Colorado flood of 2013. Figure 11 shows that the simulated peak discharge was larger and faster as precipitation increased, being 4.86 $m^3 s^{-1}$ at 1200 h 21 June, 4.27 $m^3 s^{-1}$ at 1200 h 21 June, 3.71 $m^3 s^{-1}$ at 2100 h 21 June and 3.15 $m^3 s^{-1}$ at 2200 h 21 June for precipitation increases of 100%, 75%, 50% and 25%, respectively. For the precipitation decrease, peak discharge was initially smaller and later—precipitation decreases of 25% and 50% resulted in predicted peak discharge of 2.03 $m^3 s^{-1}$ and 1.21 $m^3 s^{-1}$, both occurring at 2300 h 21 June; they were 21% and 53% lower than that of the reference precipitation. When reducing the precipitation by 75%, the predicted peak discharge during the event period was 0.56 $m^3 s^{-1}$ at 1100 h 24 June, a 78%

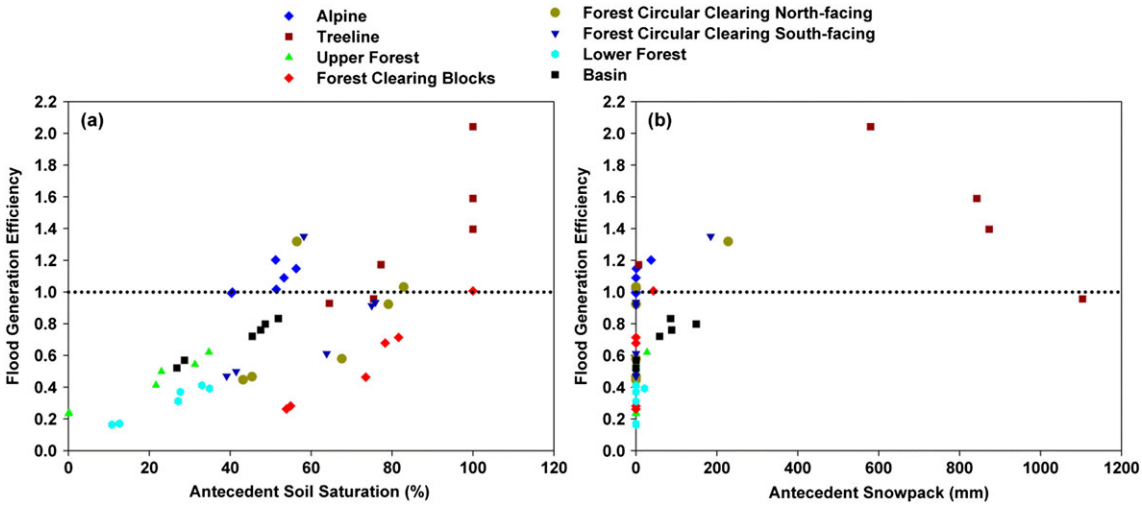

Figure 9. Scatter plots of the flood generation efficiency (FGE) and antecedent conditions from flood simulations of six different time periods in 2013: (a) antecedent soil saturation and (b) antecedent snowpack. Note FGE is the flood runoff divided by event precipitation of 250 mm and the black dotted line denotes FGE = 1

Table VI. Pearson correlation coefficient r for correlation between the flood generation efficiency (FGE) and antecedent conditions: soil saturation, and snowpack as well as correlation between the FGE and storage change from flood simulations of six different time periods in 2013

	Alpine	Treeline	Upper Forest	Forest Clearing Blocks	Forest Circular Clearing North-facing	Forest Circular Clearing South-facing	Lower Forest	Marmot Creek Basin	Below Treeline	Treeline and Alpine
Antecedent soil saturation	0.71	**0.86**	**0.99**	**0.96**	0.49	0.52	**0.98**	**0.99**	**0.69**	**0.85**
Antecedent snowpack	0.74	0.22						**0.89**		0.22
Storage change	−0.50	−0.47	**−0.87**	**−0.99**	−0.17	−0.32	**−0.87**	**−0.85**	**−0.55**	−0.47

Note: the **bold** values are statistically significant using two-tailed test with significance level of 0.05.

drop when comparing to the peak discharge with reference precipitation; this is no longer the seasonal peak discharge which was 0.62 $m^3 s^{-1}$ at 0500 h 3 July. When decreasing the precipitation by 100%, discharge steadily dropped from 0.29 $m^3 s^{-1}$ at 1300 h 17 June to 0.18 $m^3 s^{-1}$ at 2200 h 23 June, and the predicted seasonal peak discharge was much earlier, 0.62 $m^3 s^{-1}$ at 0900 h 1 June. This suggests that 2013 would have been a low flow year similar to 2009 if the June flood had not taken place.

Figure 12(a) and (b) shows the simulated FGE and its change associated with varying precipitation magnitude for all ecozones and the whole basin. FGE at the treeline ecozone was greater than 1.0, suggesting a role for ROS and snowmelt in enhancing runoff generation; here it responded inversely to the precipitation changes, meaning the ROS and snowmelt runoff generation efficiency diminishes with increasing precipitation because of a relatively invariant contribution from snowmelt with increasing precipitation. Nonetheless, the treeline ecozone forms hot spots for flood generation in the basin as it always generates more runoff than the incident precipitation. The FGE from other ecozones remained relatively constant with varying precipitation magnitude and was less than or equal to 1.0, which suggests that FGE is insensitive to precipitation magnitude and rainfall–runoff is the mechanism for generating runoff regardless of the precipitation magnitude during the flood. Figure 12(c) illustrates the change in peak hourly discharge associated with change in precipitation magnitude for all ecozones and the entire basin. The peak hourly discharge for the alpine ecozone responded greatly with changing precipitation magnitude, while for other ecozones it was relatively insensitive to varying precipitation magnitude. This is likely because of the high celerity response to flood precipitation owing to the low permeability of rock surface cover and lack of surface and subsurface storage above bedrock in the alpine

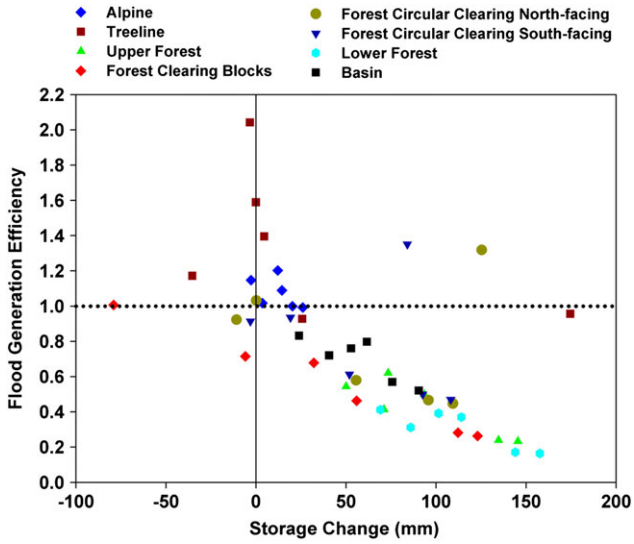

Figure 10. Scatter plots of the flood generation efficiency (FGE) and subsurface storage change from flood simulations of six different time periods in 2013. Note FGE is the flood runoff divided by event precipitation of 250 mm and the black dotted line denotes FGE = 1

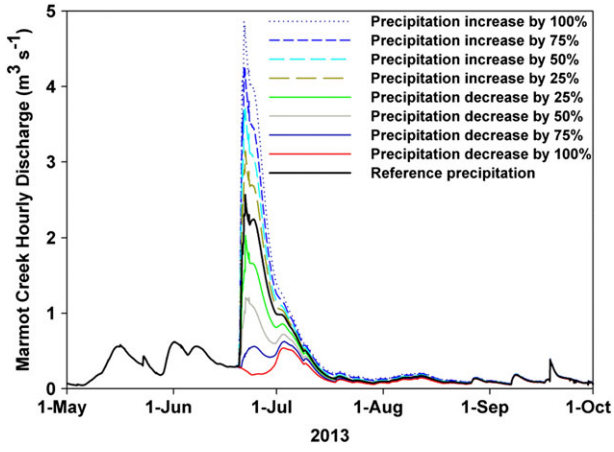

Figure 11. Hourly basin discharge from flood simulations of varying precipitation during 17–24 June 2013. Note the reference precipitation was approximately 250 mm for the basin

ecozone. The relationship between FGE and change in subsurface storage for all ecozones and the entire basin was also examined. Figure 12(d) shows FGE at the treeline ecozone ranged between 1.5 and 4.7 as precipitation varied; however, there was very little variation in subsurface storage as it was already saturated before the flood. FGE for the other ecozones below treeline was relatively constant and less than 1.0 given the wide range of storage change from −2 mm to 283 mm, which is explained by large available subsurface storage before the flood. FGE at the alpine ecozone approximately equals 1.0, which is attributed to shallow subsurface storage change ranging from −8 mm to 75 mm with varying precipitation magnitude.

Flood simulation of reduced forest canopy and soil moisture storage capacity

Hourly streamflow discharge for Marmot Creek basin during hydrological year 2012–2013 was simulated for a reduced forest canopy and soil moisture storage capacity (Figure 13). There were negligible effects on the peak discharge and flow volume during the June 2013 flood when removing all forest canopy cover in the basin. However, when forest canopy removal was accompanied by substantial soil compaction (i.e. 50% reduction in soil moisture storage capacity), both peak flood discharge and total flood discharge volume increased by 121% and 21%, respectively, compared to those from current forest cover and soil storage capacity.

DISCUSSION

The CRHM model showed adequate capability in simulating hydrology at MCRB based on streamflow evaluations over eight hydrological years from 2005 to 2013. Unfortunately, the gauging station (05BF016) at basin outlet was severely damaged during the June 2013 flood, so a rigorous streamflow evaluation during the flood was not possible, and there is uncertainty in model performance under the extreme flooding condition.

Flood simulations of ‘same time, different year’ and ‘different time in 2013’ involved substituting the flood meteorology to the same time period in other years or switching the flood meteorology with meteorology in different time periods in 2013, while holding constant the meteorological conditions prior to substitution and switch. The flood meteorology includes air temperature, relative humidity, wind speed, incoming shortwave radiation and ground surface temperature along with flood precipitation during the period of 17–24 June 2013; much of this period was warm and characteristic of summer meteorology near the summer solstice. Substitution of this particular summer meteorology to the same period in other years should not cause any inconsistencies with the original meteorology and daylight period. However, when switching the flood meteorology into spring conditions in May, the warmer air and ground surface temperatures and higher incoming shortwave radiation are no longer characteristic and may lead to disruptive changes in meteorology. These would be characteristic of a rapid warming because of advection of energy from a particularly strong frontal system. Switching the flood meteorology with that in post-flood summer periods in July avoids two consecutive floods in the same year and is a less disruptive examination of the efficiency of flood generation for different antecedent conditions than the switch with spring conditions. One of the interesting findings in ‘same time, different year’

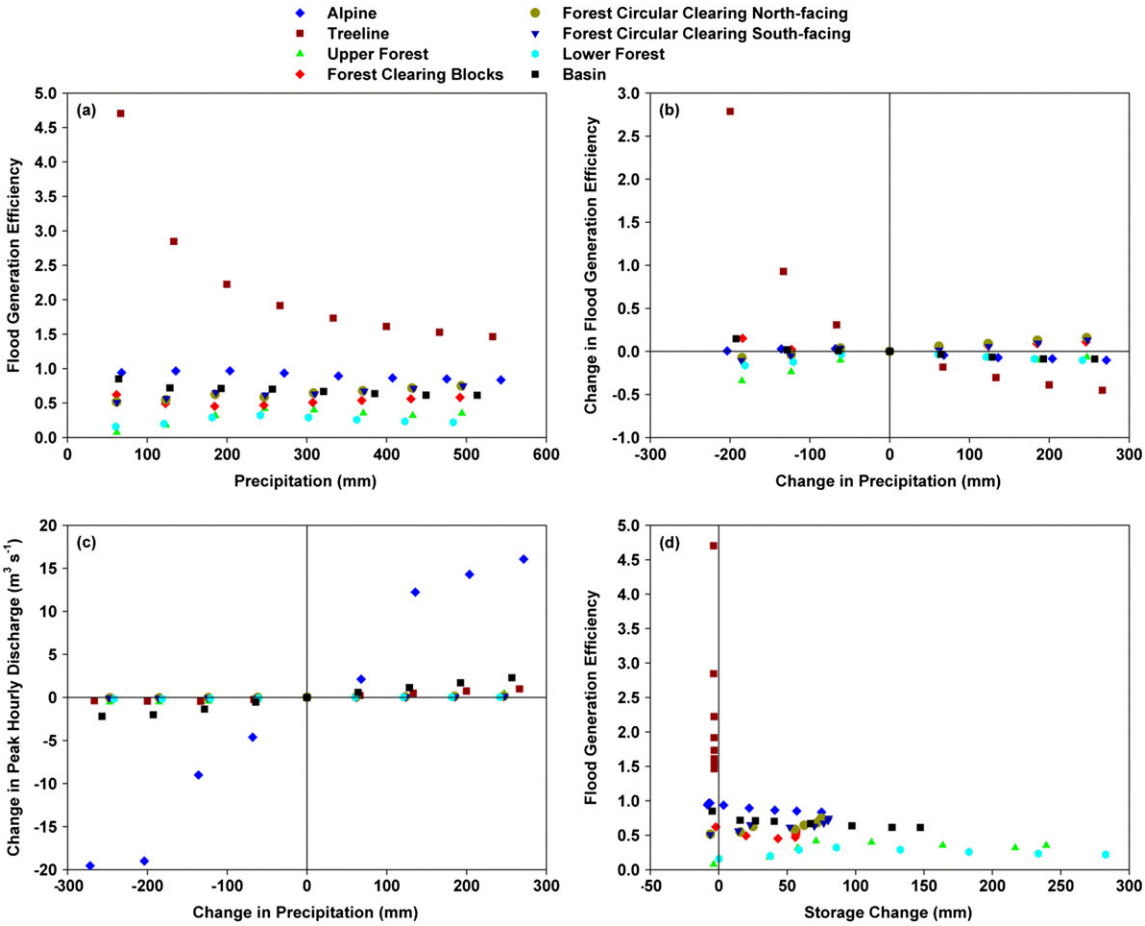

Figure 12. Scatter plots of flood simulations of varying precipitation magnitude during 17–24 June 2013: (a) flood generation efficiency (FGE) and total precipitation, (b) FGE and change in precipitation, (c) change in peak hourly discharge and change in precipitation and (d) total subsurface storage change and FGE

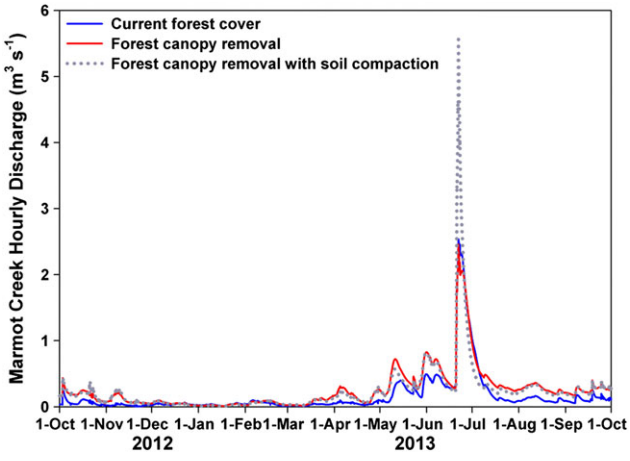

Figure 13. Hourly basin discharge from flood simulations of varying canopy cover and soil moisture storage capacity

flood simulations is that in all years examined, the flood magnitude would have been much larger than the actual one occurring in 2013. This is because of the higher basin antecedent soil moisture in other years compared to that in 2013, despite the larger basin antecedent snowpack in 2013 than that in four other years (e.g. 2006–2009). This suggests that for a late June flood, the basin antecedent soil moisture is perhaps a better indicator for the flood magnitude than the basin antecedent snowpack.

The results from this study are in general agreement with other findings about relationships between flood generation and antecedent soil moisture status, snow accumulation and air temperature (Leathers *et al.,* 1998; Rannie, 2016; Stadnyk *et al.,* 2016; Tramblay *et al.,* 2010; Wazney and Clark, 2016). Throughout the analysis of antecedent conditions, FGE generally exhibited positive relationships with antecedent precipitation and antecedent soil saturation and negative relationships with antecedent air temperature, while FGE was positively related to antecedent snowpack. The analysis of spatial variability of FGE also indicates that runoff generation was most efficient in forest clearings, treeline and alpine ecozones, and both the lower and upper elevation forest ecozones were not efficient sites of runoff generation. Difference in FGE under snow-free conditions between

the forest and forest clearing ecozones is attributed to greater subsurface storage availability in the forest, which is explained by greater evapotranspiration and intercepted snow sublimation losses from the forest leading to lower antecedent soil moisture than that in the clearings. Higher antecedent snowpacks in forest clearings is an additional contributing factor for differences in FGE under snowcovered conditions when ROS occurs. This is consistent with findings from winter ROS studies in more temperate climates (Harr, 1981; Marks *et al.,* 1998). Compared to forest ecozones, the higher values of FGE for the alpine and treeline ecozones are mainly because of a substantive antecedent snowpack and high antecedent soil saturation, resulting in ROS and snowmelt generated flood over saturated soils. The forest clearings, alpine and treeline ecozones yield more runoff than incident precipitation because of contributions from snowmelt during ROS and form runoff generation 'hotspots' in the basin; the 'hotspots' develop in the forest clearings and alpine area when the flood occurs in spring and at the treeline when it occurs in summer. Over the basin, the results showed that FGE was reduced in late June 2013; an early June flood would have generated larger volume (+15%), and an early May flood would have generated higher peak discharge (+13%). Although the results showed that 'hotspots' such as forest clearings could generate more runoff in spring leading to higher flood water yields with greater cleared area, consistent with modelling forest removal effects on peak flow in spring (Pomeroy *et al.,* 2012), heavy rainfall events in May have been relatively rare so far in the region (Harder *et al.,* 2015; Liu *et al.,* 2016; Whitfield and Pomeroy, 2016). This helps to explain why forest management practices such as clear-cutting caused small or no impact on peak streamflow or timing at Marmot Creek (Harder *et al.,* 2015; Neill, 1980). However, the risk of flooding in spring is estimated to increase with further climate change as spring rainfall magnitude and frequency increases (Farjad *et al.,* 2015; Valeo *et al.,* 2007), and historical examinations show increasing spring streamflow in the region over time (Whitfield and Pomeroy, 2016).

The results from flood simulations of varying precipitation magnitude during the 2013 flood show the FGE at treeline was consistently greater than 1.0 regardless of the precipitation magnitude. This was because of snowmelt contributions during ROS runoff generation and saturated antecedent soil moisture conditions. As precipitation volumes increased, the role of antecedent snowpack and soil saturation in ROS runoff mechanism diminished. For instance, the FGE for the alpine ecozone is close to 1.0 for any precipitation volume suggesting peak flood discharge scales with precipitation magnitude. This is associated with the lack of subsurface storage above bedrock and some exposed and steep rock surfaces resulting in a fast runoff response to rainfall with extremely small abstractions. In contrast, FGE remained relatively constant at less than 1.0 with varying precipitation volume for the forest ecozones. These ecozones were not flood generation 'hotspots' because of low antecedent soil saturation and large available subsurface storage and demonstrate why heavy precipitation events do not always result in high runoff and should not be taken as proxy for flooding (Ivancic and Shaw, 2015). For the simulation which increased precipitation by 100%, to about 500-mm total precipitation, it is difficult to estimate return interval of such a precipitation given the limited number of years of precipitation observation in the basin. The purpose of this precipitation volume sensitivity examination is to show how large the flood could be for this Canadian Rockies headwater basin with a precipitation magnitude (i.e. >450 mm) similar to that experienced in the 'Great Colorado Flood' of September 2013 (Gochis *et al.,* 2015).

The results from flood simulations of changing forest canopy and soil moisture storage capacity show that removing all forest canopy alone had minimal impacts on peak flood discharge and flow volume. This simulation might be similar to impacts of forest disease or low intensity wildfire (Fauria and Johnson, 2006, 2008; Whitfield and Pomeroy, 2016; Winkler *et al.,* 2014), and the results are very different from an examination of peak flow change with forest cover removal when peak flows are because of spring snowmelt (Pomeroy *et al.,* 2012). The difference between this forest rainfall–runoff event and a snowmelt event is most likely because of the flood precipitation being two orders of magnitude greater than typical canopy interception storage capacities and the rainfall–runoff mechanisms that were dominant in the forested ecozones which differ from the snowmelt runoff mechanisms examined by Pomeroy *et al.* (2012). However, in the simulation where forest canopy removal was accompanied with simulated overall soil compaction in which storage capacity was reduced in a spatially even manner by 50%, the peak flood discharge doubled. This combined forest and soil change simulation might be more similar to the impact of forest clear-cutting operations where heavy machinery can compact soils (Putz *et al.,* 2003; Startsev and McNabb, 2000), but it is difficult to conclude that the 50% reduction in soil moisture storage capacity would be a typical value because of compaction in the basin. The purpose of this simulation is to demonstrate the sensitivity of the flood flows to changes in forest cover and soil storage. Further, a logged basin would likely have extensive skidding road network that could alter routing patterns (King and Tennyson, 1984; Thomas and Megahan, 1998), which are not represented in the current model. Full examination of forest cover removal and soil compaction coupled over a

full range of antecedent conditions of air temperature, precipitation, snowpack and soil saturation is not within scope of this paper, so caution should be taken when interpreting results of effect of forest cover removal on flood runoff.

CONCLUSIONS

A physically based hydrological model was set up using the CRHM platform to simulate flood generation processes at Marmot Creek Research Basin during the June 2013 flood. Approximately 250 mm of precipitation fell in the basin during the flood, and the model estimated just over 250-mm runoff from the alpine ecozone of which 21% was ROS and had a snowmelt contribution, 510-mm runoff from the treeline ecozone which was completely ROS with substantial snowmelt contributions and 145-mm runoff or less from montane forest and forest clearing ecozones that was largely rainfall generated. Alpine and treeline ecozones covering 45% of the basin area contributed a disproportionate 72% of basin flow volume during the flood. At end of the flood, modelled subsurface storage peaked at levels of from 45% to 80% of saturation in forest and small forest clearing ecozones and was completely filled in both treeline and large forest clearing ecozones. 'Virtual flood' simulations showed that the FGE was lower in 2013 than in any of the seven previous years; FGE was lower in late June when the flood occurred compared to May and early June with higher peak discharges and larger flow volumes. This is because of relatively dry and/or low snowpack antecedent conditions in late June 2013. Runoff generation 'hotspots' because of rain-on-snow flooding developed in the forest clearing and alpine ecozones for simulations of the flood meteorology in early May and in the treeline ecozone for simulations of the meteorology in late June. The alpine ecozone was always an efficient generator of runoff; however, montane forests were not efficient zones of flood runoff generation under any scenario of timing or antecedent condition. Removal of the forest canopy had no influence on flood streamflow peak or volume, but compaction of soils along with removal of the forest canopy doubled the streamflow peak under the June 2013 meteorological conditions. More research is needed to fully understand the impact of forest cover change on floods in different seasons. Marmot Creek has highly heterogeneous distribution of land covers and a large elevation gradient; the magnitude and severity of floods in such a basin are closely related to the flood precipitation volume and the spatial distribution of antecedent snowpack, and storage in soils and the subsurface. Better understanding of the interaction of the spatial distribution and temporal evolution of precipitation, snowmelt and storage over the basin is key to improved understanding and prediction of the dynamics of extreme flooding events in mountains.

ACKNOWLEDGEMENTS

The authors would like to gratefully acknowledge the funding assistance provided from the Alberta Government departments of Environment and Parks, and Agriculture and Forestry, the IP3 Cold Regions Hydrology Network of the Canadian Foundation for Climate and Atmospheric Sciences, the Natural Sciences and Engineering Research Council of Canada through Discovery Grants, Research Tools and Instrument Grants, Alexander Graham Bell Scholarships and the Changing Cold Regions Network, University of Saskatchewan Global Institute for Water Security and the Canada Research Chairs programme. Logistical assistance was received from the Biogeoscience Institute, University of Calgary and the Nakiska Ski Area. Streamflow data from the Water Survey of Canada is gratefully acknowledged. Field work by many graduate students in and collaborators with the Centre for Hydrology and research officers Michael Solohub, May Guan and Angus Duncan was essential in accurate data collection in adverse conditions. Discussion about statistical analysis with Paul Whitfield was useful for developing this paper. Comments of the editor and two anonymous reviewers were greatly appreciated.

REFERENCES

Band LE. 1993. Effect of land surface representation on forest water and carbon budgets. *Journal of Hydrology* **150**: 749–772.

Beaudry P, Golding DL. 1983. Snowmelt during rain on snow in coastal British Columbia. *Proceedings of the 50th Annual Western Snow Conference*, 19–21 April 1983, Vancouver, British Columbia, 55–66.

Beke GJ. 1969. Soils of three experimental watersheds in Alberta and their hydrological significance. Ph.D. thesis, Department of Soil Science, University of Alberta, Edmonton, 456.

Bruce JP, Clark RH. 1965. *Introduction to hydrometeorology*. Pergamon Press: Toronto; 319.

Buttle JM, Allen DM, Caissie D, Davison B, Hayashi M, Peters DL, Pomeroy JW, Simonovic S, St-Hilaire A, Whitfield PH. 2016. Flood processes in Canada: regional and special aspects. *Canadian Water Resources Journal* **41**(1–2): 7–30. DOI:10.1080/07011784.2015.1131629

DeBeer CM, Pomeroy JW. 2009. Modelling snow melt and snowcover depletion in a small alpine cirque, Canadian Rocky Mountains. *Hydrological Processes* **23**: 2584–2599. DOI:10.1002/hyp.7346

DeBeer CM, Pomeroy JW. 2010. Simulation of the snowmelt runoff contributing area in a small alpine basin. *Hydrology and Earth System Sciences* **14**: 1205–1219. DOI:10.5194/hess-14-1205-2010

Dumanski S, Pomeroy JW, Westbrook CJ. 2015. Hydrological regime changes in a Canadian Prairie basin. *Hydrological Processes* **29**: 3893–3904. DOI:10.1002/hyp.10567

Ellis CR, Pomeroy JW. 2007. Estimating sub-canopy shortwave irradiance to melting snow on mountain slopes. *Hydrological Processes* **21**: 2581–2597. DOI:10.1002/hyp.6794

Ellis CR, Pomeroy JW, Brown T, MacDonald J. 2010. Simulation of snow accumulation and melt in needleleaf forest environments. *Hydrology and Earth System Sciences* **14**: 925–940. DOI:10.5194/hess-14-925-2010

Ellis CR, Pomeroy JW, Essery RLH, Link TE. 2011. Effects of needleleaf forest cover on radiation and snowmelt dynamics in the Canadian Rocky Mountains. *Canadian Journal of Forest Research* **41**: 608–620. DOI:10.1139/X10-227

Ellis CR, Pomeroy JW, Link TE. 2013. Modeling increases in snowmelt yield and desynchronization resulting from forest gap thinning treatments in a northern mountain catchment. *Water Resources Research* **49**: 936–949. DOI:10.1002/wrcr.20089

Fang X, Pomeroy JW, Ellis CR, MacDonald MK, DeBeer CM, Brown T. 2013. Multi-variable evaluation of hydrological model predictions for a headwater basin in the Canadian Rocky Mountains. *Hydrology and Earth System Sciences* **17**: 1635–1659. DOI:10.5194/hess-17-1635-2013

Farjad B, Gupta A, Marceau DJ. 2015. Hydrological regime responses to climate change for the and 2050s periods in the Elbow River Watershed in Southern Alberta, Canada. In *Environmental management of river basin ecosystems*, Ramkumar M, Kumaraswamy K, Mohanraj R (eds). Springer International Publishing: Switzerland; 65–89.

Fauria MM, Johnson EA. 2006. Large-scale climatic patterns control large lightning fire occurrence in Canada and Alaska forest regions. *Journal of Geophysical Research* **111**: G04008. DOI:10.1029/2006JG000181

Fauria MM, Johnson EA. 2008. Climate and wildfires in the North American boreal forest. *Philosophical Transactions of the Royal Society B* **363**: 2317–2329.

Garvelmann J, Pohl S, Weiler M. 2015. Spatio-temporal controls of snowmelt and runoff generation during rain-on-snow events in a mid-latitude mountain catchment. *Hydrological Processes* **29**: 3649–3664. DOI:10.1002/hyp.10460

Gochis D, Schumacher R, Friedrich K, Doesken N, Kelsch M, Sun J, Ikeda K, Lindsey D, Wood A, Dolan B, Matrosov S, Newman A, Mahoney K, Rutledge S, Johnson R, Kucera P, Kennedy P, Sempere-Torres D, Steiner M, Roberts R, Wilson J, Yu W, Chandrasekar V, Rasmussen R, Anderson A, Brown B. 2015. The Great Colorado Flood of September 2013. *Bulletin of the American Meteorological Society* **96**: 1461–1487. DOI:10.1175/BAMS-D-13-00241.1

Golding DL, Swanson RH. 1986. Snow distribution patterns in clearings and adjacent forest. *Water Resources Research* **22**: 1931–1940.

Granger RJ, Gray DM. 1989. Evaporation from natural non-saturated surfaces. *Journal of Hydrology* **111**: 21–29.

Harder P, Pomeroy JW, Westbrook CJ. 2015. Hydrological resilience of a Canadian Rockies headwaters basin subject to changing climate, extreme weather, and forest management. *Hydrological Processes* **29**: 3905–3924. DOI:10.1002/hyp.10596

Harr RD. 1981. Some characteristics and consequences of snowmelt during rainfall in western Oregon. *Journal of Hydrology* **53**: 277–304.

Hunsaker CT, Whitaker TW, Bales RC. 2012. Snowmelt runoff and water yield along elevation and temperature gradients in California's southern Sierra Nevada. *Journal of the American Water Resources Association* **48**(4): 667–678. DOI:10.1111/j.1752-1688.2012.00641.x

Ivancic TJ, Shaw SB. 2015. Examining why trends in very heavy precipitation should not be mistaken for trends in very high river discharge. *Climatic Change* **133**: 681–693. DOI:10.1007/s10584-015-1476-1

Jeffrey WW. 1965. Experimental watersheds in the Rocky Mountains, Alberta, Canada. *Proceedings of the Symposium on Representative and Experimental Areas*, IAHS Publication No. 66, 502–521.

de Jong C. 2013. Linking ICT and society in early warning and adaptation to hydrological extremes in mountains. *Natural Hazards and Earth System Sciences* **13**: 2253–2270. DOI:10.5194/nhess-13-2253-2013

King JG, Tennyson LC. 1984. Alteration of streamflow characteristics following road construction in North Central Idaho. *Water Resources Research* **20**(8): 1159–1163.

Kirby CL, Ogilvy RT. 1969. The forests of Marmot Creek watershed research basin. Canadian Forestry Service Publication No. 1259, Canadian Department of Fisheries and Forestry, Canadian Forestry Service, Ottawa, 37.

Kron W. 2005. Flood risk = hazard · values · vulnerability. *Water International* **30**: 58–68. DOI:10.1080/02508060508691837

Lawford RG, Prowse TD, Hogg WD, Warkentin AA, Pilon PJ. 1995. Hydrometeorological aspects of flood hazards in Canada. *Atmosphere–Ocean* **33**: 303–328. DOI:10.1080/07055900.1995.9649535

Leathers DJ, Kluck DR, Kroczynski S. 1998. The severe flooding event of January 1996 across north-central Pennsylvania. *Bulletin of the American Meteorological Society* **79**(5): 785–797.

Liu A, Mooney C, Szeto K, Theriault J, Kochubajda B, Stewart R, Boodoo S, Goodson R, Li Y, Pomeroy JW. 2016. The June 2013 Alberta catastrophic flooding event: Part 1—climatological aspects and hydrometeorological features. *Hydrological Processes*. DOI:10.1002/hyp.10906

Lundquist JD, Cayan DR. 2007. Surface temperature patterns in complex terrain: daily variations and long-term change in the central Sierra Nevada, California. *Journal of Geophysical Research* **112**: D11124. DOI:10.1029/2006JD007561

MacDonald MK, Pomeroy JW, Pietroniro A. 2010. On the importance of sublimation to an alpine snow mass balance in the Canadian Rocky Mountains. *Hydrology and Earth System Sciences* **14**: 1401–1415. DOI:10.5194/hess-14-1401-2010

Marks D, Kimball J, Tingey D, Link T. 1998. The sensitivity of snowmelt processes to climate conditions and forest cover during rain-on-snow: a case study of the 1996 Pacific Northwest flood. *Hydrological Processes* **12**: 1569–1587.

Marks D, Winstral A, Reba M, Pomeroy J, Kumar M. 2013. An evaluation of methods for determining during-storm precipitation phase and the rain/snow transition elevation at the surface in a mountain basin. *Advances in Water Resources* **55**: 98–110. DOI:10.1016/j.advwatres.2012.11.012

Marsh CB, Pomeroy JW, Spiteri RJ. 2012. Implications of mountain shading on calculating energy for snowmelt using unstructured triangular meshes. *Hydrological Processes* **26**: 1767–1778. DOI:10.1002/hyp.9329

Mazurkiewicz AB, Callery DG, McDonnell JJ. 2008. Assessing the controls of the snow energy balance and water available for runoff in a rain-on-snow environment. *Journal of Hydrology* **354**: 1–14.

McCabe GJ, Clark MP, Hay LE. 2007. Rain-on-snow events in the western United States. *Bulletin of the American Meteorological Society* **88**: 319–328.

Melone AM. 1985. Flood producing mechanisms in coastal British Columbia. *Canadian Water Resources Journal* **10**(3): 46–64. DOI:10.4296/cwrj1003046

Monteith JL. 1965. Evaporation and environment. In *State and movement of water in living organisms. 19th Symposium of the Society for Experimental Biology*. Cambridge University Press: Cambridge; 205–234.

Musselman KN, Molotch NP, Brooks PD. 2008. Effects of vegetation on snow accumulation and ablation in a mid-latitude sub-alpine forest. *Hydrological Processes* **22**: 2767–2776. DOI:10.1002/hyp.7050

Nash JE, Sutcliffe JV. 1970. River flow forecasting through conceptual models. Part I—A discussion of principles. *Journal of Hydrology* **10**: 282–290.

Neill CR. 1980. Forest management for increased water yield—how useful in Southern Alberta. *Canadian Water Resources Journal* **5**: 56–75.

Newton B, Burrell BC. 2016. The April–May 2008 flood event in the Saint John River Basin: causes, assessment and damages. *Canadian Water Resources Journal* **41**(1–2): 118–128 DOI:10.1080/07011784.2015.1009950

Pomeroy JW, Gray DM, Brown T, Hedstrom NR, Quinton W, Granger RJ, Carey S. 2007. The Cold Regions Hydrological Model, a platform for basing process representation and model structure on physical evidence. *Hydrological Processes* **21**: 2650–2667. DOI:10.1002/hyp.6787

Pomeroy JW, Marks D, Link T, Ellis C, Hardy J, Rowlands A, Granger R. 2009. The impact of coniferous forest temperature on incoming longwave radiation to melting snow. *Hydrological Processes* **23**: 2513–2525. DOI:10.1002/hyp.7325

Pomeroy J, Fang X, Ellis C. 2012. Sensitivity of snowmelt hydrology in Marmot Creek, Alberta, to forest cover disturbance. *Hydrological Processes* **26**: 1892–1905. DOI:10.1002/hyp.9248

Pomeroy JW, Fang X, Shook K, Whitfield PH. 2013. Predicting in ungauged basins using physical principles obtained using the deductive, inductive, and abductive reasoning approach. In *Putting prediction in ungauged basins into practice*, Pomeroy JW, Whitfield PH, Spence C (eds). Canadian Water Resources Association: Canmore, Alberta; 41–62.

Pomeroy JW, Shook K, Fang X, Dumanski S, Westbrook C, Brown T. 2014. Improving and Testing the Prairie Hydrological Model at Smith Creek Research Basin. Centre for Hydrology Report No. 14, University of Saskatchewan, Saskatoon, 102. Available online at http://www.usask.ca/hydrology/Reports.php

Pomeroy J, Stewart RE, Whitfield PH. 2016a. The 2013 flood event in the Bow and Oldman River basins: causes, assessment and damages. *Canadian Water Resources Journal* **41**(1–2): 105–117. DOI:10.1080/07011784.2015.1089190

Pomeroy JW, Fang X, Marks D. 2016b. A cold rain on snow event in the Canadian Rockies—characteristics and diagnosis. *Hydrological Processes*. DOI:10.1002/hyp.10905

Poulos MJ, Pierce JL, Flores AN, Benner SG. 2012. Hillslope asymmetry maps reveal widespread, multi-scale organization. *Geophysical Research Letters* **39**: L06406. DOI:10.1029/2012GL051283

Putz G, Burke JM, Smith DW, Chanasyk DS, Prepas EE, Mapfumo E. 2003. Modelling the effects of boreal forest landscape management upon streamflow and water quality: basic concepts and considerations. *Journal of Environmental Engineering and Science* **2**: S87–S101.

Rannie W. 2016. The 1997 flood event in the Red River basin: causes, assessment and damages. *Canadian Water Resources Journal* **41**(1–2): 45–55. DOI:10.1080/07011784.2015.1004198

Saad C, St-Hilaire A, Gachon P, El Adlouni S. 2016. The 2011 flood event in the Richelieu River basin: causes, assessment and damages. *Canadian Water Resources Journal* **41**(1–2): 129–138. DOI:10.1080/07011784.2014.999825

Sandink D, Kovacs P, Oulahen G, McGillivray G. 2010. Making Flood Insurable for Canadian Homeowners: A Discussion Paper. Institute for Catastrophic Loss Reduction & Swiss Reinsurance Company Ltd., Toronto, 75.

Shook K. 2016. The 2005 flood events in the Saskatchewan River Basin: causes, assessment and damages. *Canadian Water Resources Journal* **41**(1–2): 94–104. DOI:10.1080/07011784.2014.1001439

Shook K, Pomeroy J. 2012. Changes in the hydrological character of rainfall on the Canadian prairies. *Hydrological Processes* **26**: 1752–1766. DOI:10.1002/hyp.9383

Simonovic SP. 2014. Through hell and high water!. *Journal of Flood Risk Management* **7**: 1–2. DOI:10.1111/jfr3.12104

Stadnyk T, Dow K, Wazney L, Blais E. 2016. The 2011 flood event in the Red River Basin: causes, assessment and damages. *Canadian Water Resources Journal* **41**(1–2): 65–73. DOI:10.1080/07011784.2015.1008048

Startsev AD, McNabb DH. 2000. Effects of skidding on forest soil infiltration in west-central Alberta. *Canadian Journal of Soil Science* **80**: 617–624.

Storr D. 1967. Precipitation variation in a small forested watershed. *Proceedings of the 35th Annual Western Snow Conference*, 18-20 April 1967, Boise, Idaho; 11–17.

Thomas RB, Megahan WF. 1998. Peak flow responses to clear-cutting and roads in small and large basin, western Cascades, Oregon: a second opinion. *Water Resources Research* **34**(12): 3393–3403.

Tramblay Y, Bouvier C, Martin C, Didon-Lescot J-F, Todorovik D, Domergue J-M. 2010. Assessment of initial soil moisture conditions for event-based rainfall–runoff modelling. *Journal of Hydrology* **387**: 176–187.

Valeo C, Xiang Z, Bouchart FJ, Yeung P, Ryan MC. 2007. Climate change impacts in the Elbow River Watershed. *Canadian Water Resources Journal* **32**(4): 285–302.

Verseghy DL. 1991. CLASS-A Canadian land surface scheme for GCMs. I. soil model. *International Journal of Climatology* **11**: 111–133.

Wazney L, Clark SP. 2016. The 2009 flood event in the Red River Basin: causes, assessment and damages. *Canadian Water Resources Journal* **41**(1–2): 56–64. DOI:10.1080/07011784.2015.1009949

Whitfield PH. 2012. Floods in future climate: a review. *Journal of Flood Risk Management* **5**: 336–365. DOI:10.1111/j.1753-318X.2012.01150.x

Whitfield PH, Pomeroy JW. 2016. Changes to flood peaks of a mountain river: implications for analysis of the 2013 flood in the Upper Bow River, Canada. *Hydrological Processes* this issue

Winkler R, Boon S, Zimonick B, Spittlehouse D. 2014. Snow accumulation and ablation response to changes in forest structure and snow surface albedo after attack by mountain pine beetle. *Hydrological Processes* **28**: 197–209. DOI:10.1002/hyp.9574

Zhang M, Wei X. 2014. Contrasted hydrological responses to forest harvesting in two large neighbouring watersheds in snow hydrology dominant environment: implications for forest management and future forest hydrology studies. *Hydrological Processes* **28**: 6183–6195. DOI:10.1002/hyp.10107

